DIRECT NUMERICAL SIMULATION OF ROTATING TURBULENT DUCT FLOW

Gustaf E. Mårtensson, Geert Brethouwer and Arne V. Johansson
Department of Mechanics,
Royal Institute of Technology (KTH)
100 44 Stockholm, Sweden
gustaf@mech.kth.se, geert@mech.kth.se, viktor@mech.kth.se

ABSTRACT

A direct simulation of turbulent flow in a rotating square duct using a second-order finite-volume method was performed. The axis of rotation was normal to the direction of the mean flow in the duct. The simulations are performed at $\mathrm{Re_d} = 4400$ and for $\mathrm{Ro_d} = 0$ up to 0.77. The strong effect of rotation on both the mean axial and secondary flows is plainly exhibited. A linear increase in the magnitude of the secondary flow was found with increasing rate of rotation. Turbulence quantities are presented to shed some light on the role of the boundary layer structure on the resistance of the flow. The growth of large-scale secondary roll-cells in the axial direction is studied with reference to their dependence on the rotation number. The case of turbulent flow in a rotating duct that has been tilted 45° around the axis of the mean flow is presented to illustrate the importance of geometric constraints on the characteristics of the flow.

INTRODUCTION

The study of fluid flow in non-inertial frames of reference is of great interest to both academia and industry. Industrial applications, such as centrifugal separators, turbines and radial compressor impellers are all systems that incorporate rotating bodies of fluid. It is known that Coriolis effects in rotating flows are of primary importance not only for mean flow quantities, such as bulk velocity, but also for turbulence intensities and structures. The ability to accurately model these effects offers the possibility of increasing device performance, while shortening the time for expensive prototype development. In order to assess the accuracy of turbulence models that are developed, both carefully collected experimental and numerical data from well-defined test cases are needed. This project attempts to alleviate the lack of rigorous numerical data.

The earliest experimental study of consequence was performed by Dobner (1959). In his thesis, the case of fully developed turbulent flow was studied by evaluating pressure measurements along the length of a circular pipe and a rectangular duct. Dobner examined in depth the relation between the friction factor of the flow and Reynolds, $\mathrm{Re} = Uw/\nu$ and rotation number, $\mathrm{Ro} = \Omega w/U$, where U is the bulk fluid speed, w is the duct width, ν is the viscosity and Ω is the magnitude of the system rotation. The Reynolds number in the experiments of Dobner was between 130 and $4{\cdot}10^4$, while the rotation number Ro lay between 0 and approximately 1.

The effects of rotation on the flow in a long high aspect ratio rectangular channel was studied experimentally by Halleen (1967). Total pressure and static pressure traverses were performed and from these, velocity profiles were deduced. The data were taken at downstream positions of 58 and 68 channel widths.

In an early study of fully developed turbulent flow in an orthogonally rotating rectangular duct, Moore (1967) measured velocity profiles in two channel planes, as well as shear stresses and turbulence intensities in low aspect ratio rectangular ducts for a number of moderate rotational velocities.

An extensive study of the effects of system rotation on separation in diffusers was performed by Rothe (1975). The experiments revealed a strong correlation between the magnitude and direction of rotation and the size of the separation bubble behind the diffuser step. The authors saw a stabilization and destabilization of the separation bubble, manifested in a shorter and longer reattachment length, on the suction and pressure sides of the diffuser.

A study of fully developed turbulent flow in a high-aspect duct was performed by Johnston et al. (1972) in order to further understand the effects of rotation on two-dimensional local and global stability. Johnston et al. used bubble-generation techniques to gather mean flow profiles and indirectly calculate shear stress profiles. The authors present three major phenomena caused by rotation, namely the reduction (increase) of turbulent wall-layer streak bursting rate in locally stabilized (destabilized) layers, the total supression of turbulence production in the locally stabilized layer and the development of roll cells on the destabilized side of the channel.

In order to study longitudinal roll-cells, Wagner and Velkoff (1972) performed experiments on the turbulent flow in a rotating duct of low-aspect ratio. Although they focused on the secondary flow of the system, measurements of the mean-flow and other quantities were used to choose the appropriate measurement position for various quantities. The authors did not observe any major effects of rotation on the pressure or mean velocity of the flow in the duct.

The experimental study of Koyama and Ohuchi (1985) concerns the turbulent flow in a high ratio (7:1) rectangular duct. Hot-wire measurements were made at six different downstream positions for a number of different flow and rotation speeds. In the case of zero rotation the boundary layers developed and met in the length of the duct, which was approximately $20H$, where H is the channel half-width. Although the velocity profiles grew as expected, a study of turbulent intensities revealed that the flow was far from fully-developed. As rotation was applied and increased, the core flow obtained the characteristic linear velocity profile in the core region, while a laminar-like profile developed on the suction side.

The experimental work by Watmuff et al. (1985) focused on studying the development of turbulent boundary layers in

a rectangular duct with a 4:1 height to width ratio at rotation numbers Ro = 1.92, 1.44 and 0.96 based on the hydraulic diameter and the bulk velocities. The authors conclude that, contrary to theories based on the analogy between rotation, buoyancy and surface curvature, the deviations from non-rotating flow profiles follow a logarithmic relationship, instead of a linear dito. Turbulence quantities are seen to follow an inner and outer scaling independent of rotation, with an enhanced development on the destabilized side.

A DNS study of rotating plane channel flow driven by a constant pressure gradient at various Reynolds and rotation numbers was done by Alvelius and Johansson (1999). They also found the expected linear core of the mean flow profile and a strong rotational effect on second order statistics was detected. Despite an apparently very complicated dependence on the rotation number, accurate predictions of the wall shear stresses were obtained using the equation of total shear and a simple approximation of the mean velocity profile.

Pallares and Davidson (2000) carried out Large Eddy Simulations (LES) of channel and duct flow using the localized dynamic subgrid-scale model of low Reynolds number ($\mathrm{Re}_\tau = 300$) duct flow for Rotation numbers in the intervall $0 \leq \mathrm{Ro}_\tau \leq 1.5$. The index τ indicates that the average friction velocity u_τ was used. They obtained results for low order statistics which are in good qualitative agreement with the DNS data for the case of rotating channel flow.

A direct numerical simulation using pseudospectral methods was performed by Wu and Kasagi (2004) to investigate the influence of an arbitrary direction of rotation on the flow in a turbulent channel. The authors found that spanwise rotation has an effect over the entire channel, while streamwise rotation, although of comparable magnitude, mainly effects the suction side of the channel. A wall-normal rotational component affects the flow dramatically inducing a strong spanwise mean velocity.

Pettersson Reif and Andersson (2003) used a differential Reynolds stress closure to model the flow in a rotating square duct. The model used an elliptic relaxation technique for the pressure-strain tensor. Their results showed good agreement in the major flow features in the duct, while turbulence quantities such as the turbulent correlations were not reproduced faithfully.

In summary, it can be stated that although a considerable amount of experimental, analytical and numerical work has been performed on rotating channels and ducts, there is a need for accurate direct numerical simulations to increase our understanding of the complex phenomena tied to the rotation of fluid flows. Attempts of modelling effects of rotation are dependent on having reliable data to compare against.

SIMULATIONS

In the present study, a DNS of turbulent flow in a square duct of width w, height h and length ℓ, rotating along an axis normal to the direction of the mean flow, is carried out, see figure 1. The flow field is assumed to be fully developed and therefore periodic boundary conditions in the flow direction are used. The flow is driven by a pressure gradient.

The instantaneous equations of motion that govern the flow of an incompressible fluid in a rotating frame of reference can be expressed as follows,

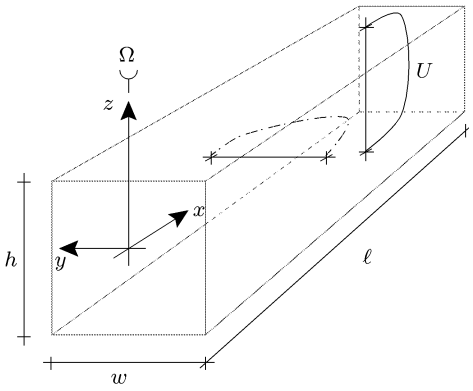

Figure 1: A schematic of the flow in a rotating duct. The asymmetric velocity profile (−·) in the xy-plane is shown, as well as the symmetric velocity profile (–) in the xz-plane.

$$\frac{\partial u_i}{\partial t} + \frac{\partial}{\partial x_j}(u_i u_j) = -\frac{1}{\rho}\frac{\partial p^*}{\partial x_i} + \nu\frac{\partial^2 u_i}{\partial x_j \partial x_j} + \\ +2\varepsilon_{ijk} u_j \Omega_k \qquad (1)$$

and

$$\frac{\partial u_j}{\partial x_j} = 0 \quad , \qquad (2)$$

where ρ is the density of the fluid, u_i denotes the instantaneous velocity in the x_i-direction, Ω_i is the rotation in the same direction and ε_{ijk} is the Levi-Civita symbol. The term p^*, known as the reduced mean static pressure, conveniently swallows the centrifugal pressure term and is expressed as

$$p^* = p - \frac{1}{2}\rho\Omega^2 \vec{r}_\perp^{\,2} \quad , \qquad (3)$$

where $\vec{r}_\perp$ is the position vector normal to the axis of rotation to a given mass element.

The system of equations 1 and 2 is discretized by means of a second-order accurate finite volume method on a staggered grid. A second-order Adams-Bashforth scheme were used for the time integration of advective and diffusive terms. For the solution of the Poisson equation for the pressure we apply a Fast Fourier Transform in the periodic direction and cyclic reduction solver for the remaining directions.

The computation is carried out for a domain of size 9.4 × 1 × 1 with 240 × 120 × 120 grid nodes in the x, y, and z direction, respectively. In order to resolve the boundary layers of the duct flow which become increasingly thin with increased rotation number, a criterion of fifteen grid points within the boundary layer has been set. The grid points are uniformly distributed in the x-direction, while the grid was refined exponentially towards the side walls of the duct in the y and z directions. The Kolmogorov length scale, λ of the flow can be estimated using the relationship $\lambda/w \sim \mathrm{Re}^{1/4} \approx 8$. The normalized wall viscous scale can be calculated as $\ell_v/L = 1/(\mathrm{Re}\sqrt{C_f}) \approx 0.01$. The first grid point in these simulations was 0.01 and 30 points resolved the boundary layer up to $l^+ = 30$.

Simulations have been performed for a set of rotation numbers between 0 and 0.77, where the rotation number based

on the width of the duct, w. The Reynolds numberwas been chosen to be 4400 in order to facilitate validation comparisons with the work of Gavrilakis (1992) for turbulent flow in a stationary duct. A comparison of major flow features for the two simulations showed good agreement.

RESULTS AND DISCUSSION

The effects of rotation on the flow in a rotating duct are so many and surprising that only some aspects of its influence are included here. The discussion will begin with mean flow quantities such as axial and secondary velocities and patterns of dito. The effect of rotation on the boundary layer configuration in the duct will follow. The discussion will continue with turbulence quantities, such as the main velocity correlations. Trends in the levels of total kinetic energy in the flow will be illuminated. The section will be concluded with the case of a tilted duct configuration, where the implications of a change of geometric constraint will be considered.

Mean flow quantities

A logical starting point for the analysis of the simulation results is with mean flow velocities. In figure 2, contours of the streamwise flow speed are presented for Ro = 0, 0.055, 0.11, 0.22, 0.43 and 0.77. The presentation of the contours in half-plots exposes the fact that the flow is symmetric around the plane normal to the axis of rotation. It is also noticed that an elongation of the contours is evident for increasing rotation number implying that the flow becomes more uniform in the z-direction. This is not surprising considering the tendency towards a columnar flow of reduced dimensionality that is characteristic for rotational flows.

As was shown in equation 1, system rotation will introduce extra acceleration terms to the equations of motion, namely the centrifugal and Coriolis terms. The Coriolis term can be seen to act as a pseudo-force in the wall-normal y-direction in the duct, in a manner similar to that caused by a density stratification, or surface curvature. The wall at $y = 0$ is therefore referred to as the pressure, or destabilized, side. The low pressure side of the duct is denoted the suction, or stabilized, side.

Using the coordinates of figure 1, it is known that a duct flow in the x-direction subjected to system rotation around the z-axis will exhibit a skewed mean velocity profile in the y-direction. Although the skewed velocity profile is present in the analogous flow case of rotating channel flow, the slope of the core region is opposite to that of the case of duct flow. The horizontal surfaces present in the duct configuration result in a non-homogeneous z-direction resulting in a secondary flow in the yz-plane. There is also a weak secondary flow in the non-rotating case, driven by the anisotropy of the turbulent stresses.

If the velocity profiles of the mean streamwise flow of the present simulations are studied, see figure 3, we see that the expected tilting of the mean streamwise velocity profile in the xy-plane was produced faithfully. The profile in the vertical xz-plane reinforces the one-dimensionalization of the flow at high rotation numbers.

Secondary flow

At Ro = 0, there exists a weak secondary flow consisting of symmetric vortex pairs in each of the corners of the duct. Due to rotation, secondary flows along the vertical and horizontal walls will develop, and with them the vertical and horizontal equivalents to Stewartsson and Ekman layers. In figures 2 and 3 b), the dominance of the rotational flow signature is evident. If the secondary components normal to the streamwise flow are studied, this is once again noticed, see figure 4.

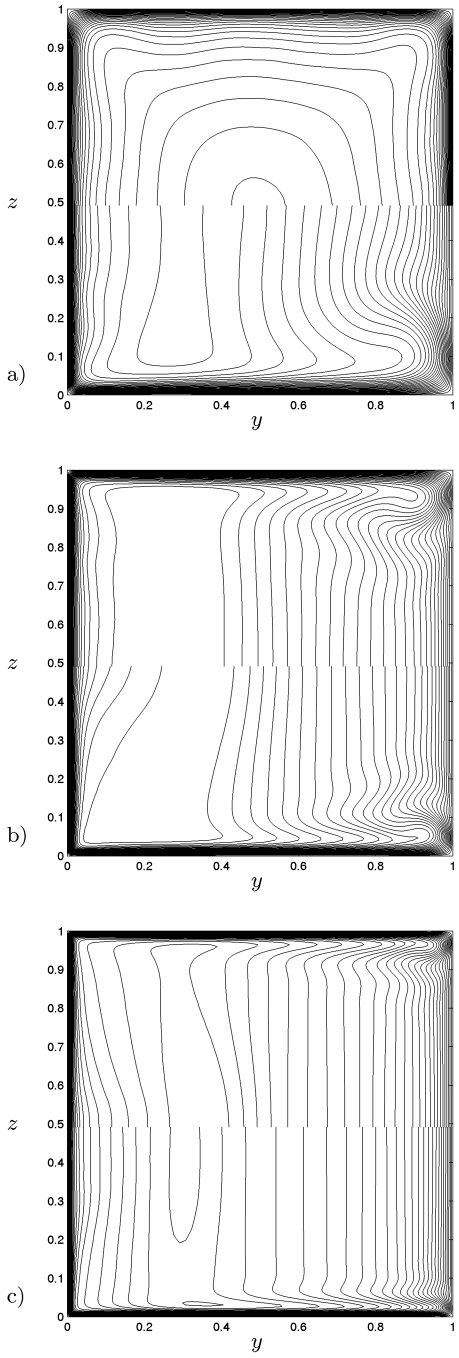

Figure 2: U_{mean}/U_b-contours for Ro = 0, 0.055, 0.11, 0.22, 0.43 and 0.77, from top to bottom. The contours span from 0 to 1.3 in increments of 0.05.

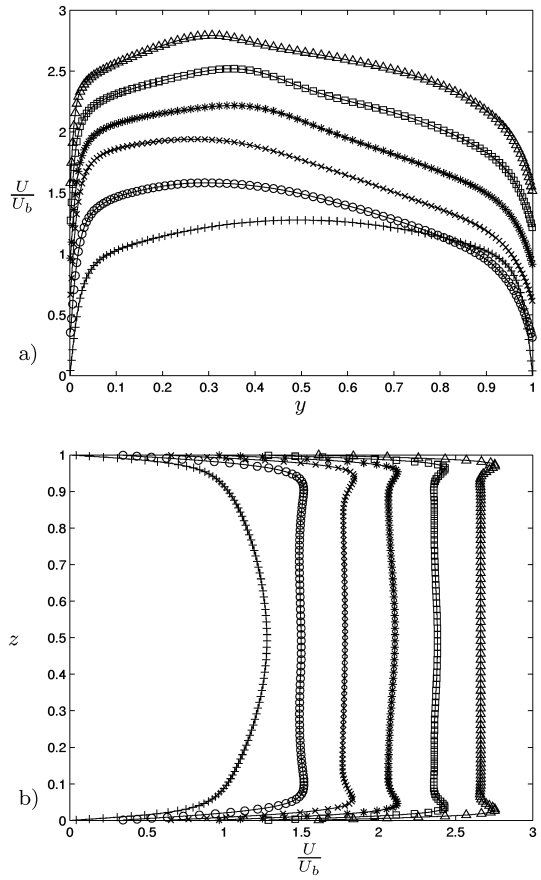

Figure 3: Velocity profiles of U_{mean}/U_b in a) the xy- and b) xz-plane for Ro = 0 (+), 0.055 (○), 0.11 (×), 0.22 (∗), 0.43 (□) and 0.77 (△). The profiles are presented for $y = z = 0.5$.

With it was discovered a linear growth of the maximum secondary velocity which was found in the turbulent equivalent of the horizontal Ekman layer. The maximum secondary flow speeds are approximately one tenth that of the streamwise flow.

In figure 4, the development of secondary vortices at Ro > 0.11 is evident. These secondary Taylor-Görtler-like vortices develop on the unstable side of the duct in a pair that is symmetric around the y-axis. It has been hypothesized that these vortices may indeed be one of the corner vortices from the non-rotational case that have developed due to turbulence interactions. The considerable growth of the vortices at Ro= 0.22 encourages further study of this feature. Due to the limited number of rotation numbers available for study, we are not able to identify the critical rotation number at which the secondary vortices develop.The studies that were performed point to $0.11 < \text{Ro}_{\text{cr}} < 0.22$. The secondary vortices grow in strength and then decrease in intensity, a reflection of the initially destabilizing effect of rotation that is changed to a stabilizing (and laminarizing) effect as Ro increases. This trend was also found in the LES study of Pallares and Davidson (2000). The maximum intensity of the secondary vortices lies at a rotation number somewhere between 0.22 and 0.77.

Mårtensson et al. (2002) found experimentally that the coefficient of friction grows with an increasing Rotation number. Evidence was given that the friction coefficient scales with the width of the duct. The DNS performed shows that the boundary layer thickness in the horizontal Ekman layers is markedly thinner than those in the vertical Stewartsson-like layers resulting in a dominating contribution to the pressure drop from the horizontal Ekman layers, supporting the width of the duct as the proper scaling length.

In figure 5, the total kinetic energy of the secondary flow integrated over the whole volume is plotted as a function of the rotation number. The total kinetic energy of the non-rotating case is naturally very small, but greater than zero. A natural increase in the kinetic energy of the secondary flow with increasing rotation number is noticed. The increase has a linear behaviour until Ro = 0.43. A slower increase is seen for higher rotation rates.

Turbulence intensities

After having noticed suggestions of the stabilizing effect of rotation at high rotation rates in the secondary flow, we turn our attention to turbulence quantities that will give us more information concerning this subject. In figure 6, contour plots of the Reynolds stress $\langle u'^2 \rangle$ show a strong dependance on rotation. As the rate of rotation increases, turbulent events are found predominantly on the pressure side of the duct, while a distinct low turbulence region is found on the suction side of the duct. High turbulence intensities are, of course, also found in the Ekman layers.

Tilted configuration

Additionally, the case of a duct that has been tilted around the direction of the mean flow was studied. This case was studied experimentally by Mårtensson et al. (2002) for the rotation angle 45° and the intuitively unexpected result of an increased friction coefficient for the tilted case compared with the standard duct configuration was found. Simulations of the same case show the formation of Ekman-like boundary layers on all four sides of the duct in this configuration, see figure 7, which may explain an increase in pressure drop for this case. It was also shown that this flow was more prone to laminarize at lower Ro, which points to a decrease in flow resistance.

In line with the reasoning of Pettersson Reif and Andersson (2003), a comparison of the streamwise flow resistance for the tilted and non-tilted configuration was carried out. Due to the fact that the Reynolds number was held constant in this study, the integrated shear stress of the duct was calculated. A decrease of 10% of the integrated shear stress was found in the tilted case which supports the modelling result of Pettersson Reif and Andersson, but contradicts the experimental findings of Mårtensson et al. (2002).

SUMMARY AND CONCLUSIONS

Direct numerical simulations of turbulent flow in a duct subjected to spanwise rotation have been performed for a number of rotation numbers. Mean flow quantities exhibit the characteristic complex three-dimensional flow properties that are expected for rotational flow. A skewing of the streamwise flow field and development of the secondary velocity field are shown to develop very rapidly. The magnitude of the secondary flow grows approximately linearly with the rotation

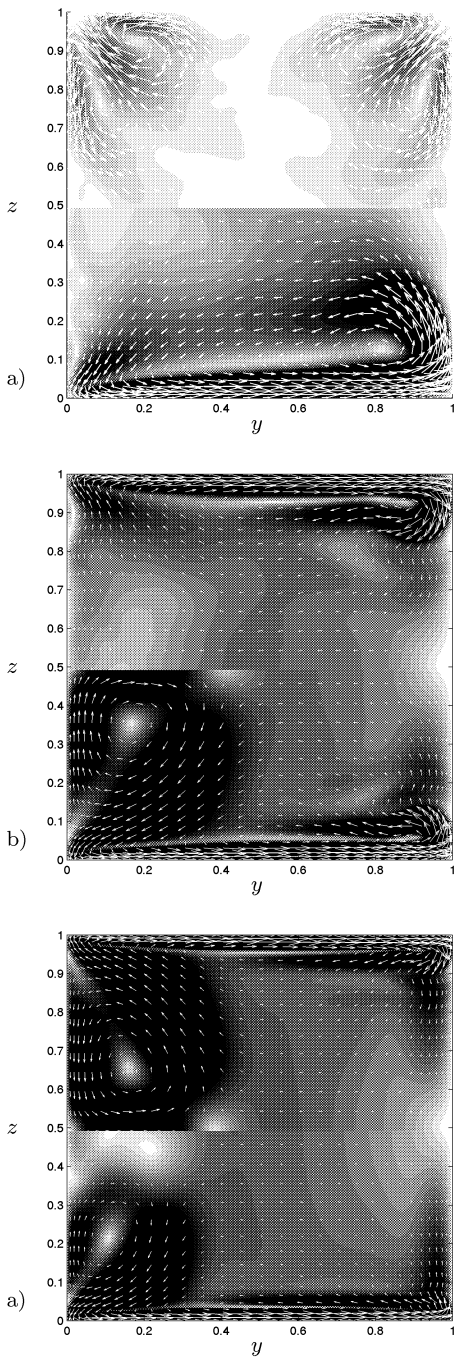

Figure 4: Contour plots of the magnitude, as well as the velocity field, of the secondary flow for Ro = 0, 0.055, 0.11, 0.22, 0.43 and 0.77, from top to bottom. The contours span from 0 to 0.032 in increments of 0.002.

number in the span of rotation numbers that were calculated. Thin Ekman-like boundary layers on the horizontal surfaces of the duct are shown to develop. These thin boundary layers are responsible for the increased pressure drop found in rotational systems compared to non-rotational systems.

A clear tendency towards stabilization of the flow is noticed through observation of the decrease in intensity of the secondary vortices as Ro increases, as well as the intensity of Reynolds stress components. Where a maximum of instability may be found has not been answered in this study.

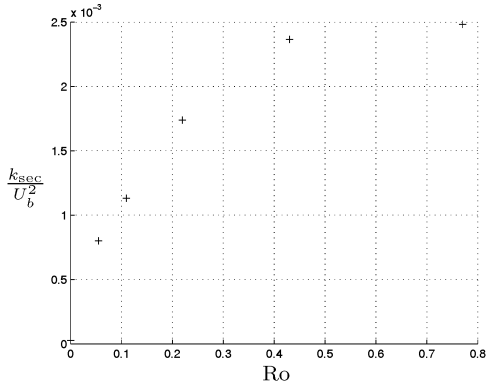

Figure 5: The total kinetic energy of the secondary flow integrated over the whole volume normalized by U_b^2 as a function of the rotation number Ro.

Calculations with a tilted duct configuration were presented. An increase in the total shear contradicts the experimental findings of Mårtensson et al. (2004) concerning an increased pressure drop in a tilted duct when compared to the non-tilted configuration.

ACKNOWLEDGMENTS

The authors would like to acknowledge the many valuable coversations that were held with Dr. Stefan Wallin, FOI and KTH.

REFERENCES

Alvelius, K. and Johansson, A.V. 1999 "Direct numerical simulation of rotating channel flow at various Reynolds numbers and Rotation numbers", Ph.D. thesis of Krister Alvelius, Dept. of Mech., Royal Inst. of Tech., Stockholm, Sweden. TRITA-MEK 1999:09, Paper 6.

Dobner, E. 1959 "Über den Strömungswiderstand in einem rotierenden Kanal", Dissertation, Technische Hochschule Darmstadt.

Gavrilakis, S. 1992 "Numerical simulation of low-Reynolds-number turbulent flow through a straight square duct", *J. Fluid Mech.*, **244**, pp. 101–129.

Halleen, R.M. and Johnston, J.P. 1967 "The influence of Rotation on Flow in a Long Rectangular Channel – An Experimental Study", Ph.D. thesis of Halleen, R.M., Stanford Univ., also Rep. MD-18, Thermosciences Div., Dept. of Mech. Engrg., Stanford University.

Johnston, J.P., Halleen, R.M. and Lezius, D.K. 1972 "Effects of spanwise rotation on the structure of two-dimensional fully developed turbulent channel flow", *J. Fluid Mech.*, **56**, pp. 533–557.

Koyama, H.S. and Ohuchi, M. 1985 "Effects of Coriolis force on boundary layer development", *Proceedings of the Fifth Symposium on Turbulent Shear Flows*, Ithaca, New York, pp. 21.19–21.24.

Moore, J. 1967 "Effects of Coriolis on Turbulent Flow in

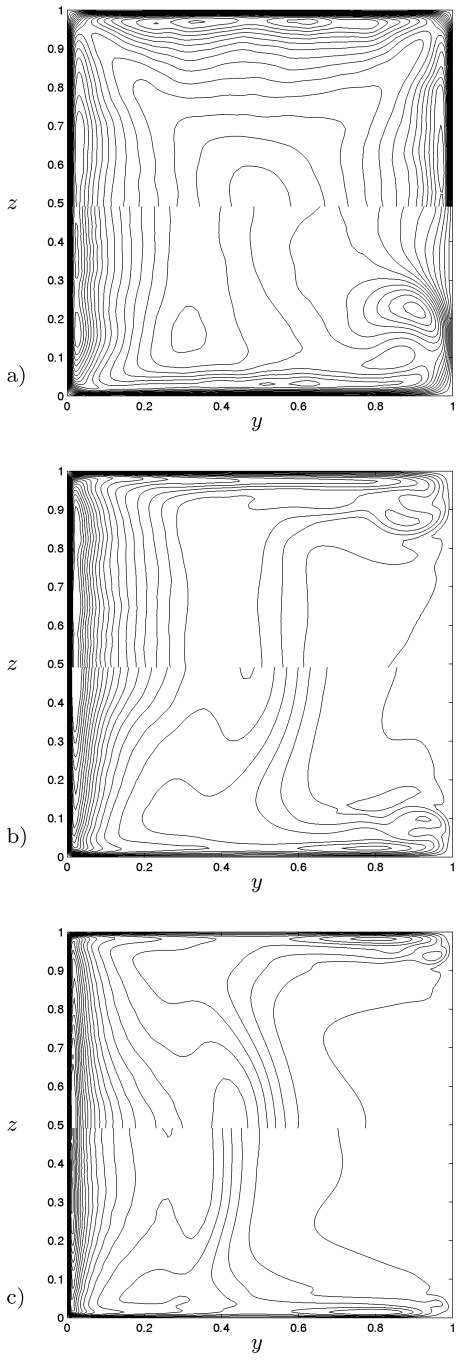

Figure 6: Contour plots of $\langle u'^2 \rangle / U_b$ for Ro = 0, 0.055, 0.11, 0.22, 0.43 and 0.77, from top to bottom. The contours span from 0 to 0.22 in increments of 0.01.

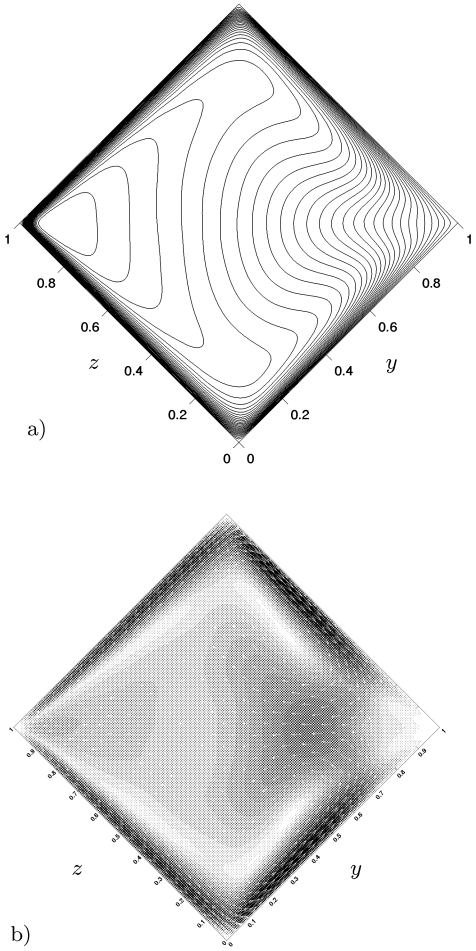

Figure 7: Plots of a) U_{mean}/U_b-contours tilted configuration ($\alpha = 45°$) and b) total kinetic energy and vector field for the secondary flow for Ro = 0.055. The contours span from 0 to 14 in increments of 0.5 for the mean velocity and from 0 to 0.15 with steps of 0.005 for the kinetic energy.

Rotating Rectangular Channels", Gas Turbine Lab Report No. 38, Mass. Inst. Tech. 1967.

Mårtensson, G.E., Gunnarsson, J., Johansson, A. V. and Moberg, H. 2002 "Experimental investigation of a rapidly rotating turbulent duct flow", *Exp. Fluids*, **33**, pp. 482–487.

Pallares, J. and Davidson, L. 2000 "Large-eddy simulations of turbulent flow in a rotating square duct", *Phys. Fluids*, **12**, n 11, pp. 2878–94.

Pettersson Reif, B.A. and Andersson, H.I. 2003 "Turbulent flow in a rotating square duct: a modelling study", *J. of Turbulence*, **4**, 012.

Rothe, P.H. 1975 "The effects of system rotation on seperation, reattachment and performance in two-dimensional diffusors", Ph.D. thesis Stanford University, Dept Mechanical Engineering.

Wagner, R.E. and Velkoff, H.R. 1972 "Measurements of Secondary Flows in a Rotating Duct", *Trans. of the ASME, Journal of Engineering for Power*, October, pp. 261–270.

Watmuff, J.H., Witt, H.T. and Joubert, P.N. 1985 "Developing turbulent boundary layers with system rotation", *J. Fluid Mech.*, **157**, pp. 405–448.

Wu, H. and Kasagi, N. 2004 "Effects of arbitrary directional system rotation on turbulent channel flow", *Phys. Fluids*, **16**, pp. 979–990.